

# AUTOMATIC CLASSIFICATION OF COMPRESSION WOOD IN GREEN SOUTHERN YELLOW PINE

*Jan Nyström*

Ph.D. Student  
Division of Wood Technology  
Luleå University of Technology  
SE 93187 Skellefteå, Sweden

and

*D. Earl Kline†*

Associate Professor  
Department of Wood Science and Forest Products  
Virginia Tech  
Blacksburg, Virginia 24061-0503, VA

(Received June 1999)

## ABSTRACT

Compression wood is a feature in softwoods that is undesired in sawn wood products due to its tendency to bend and crook as the moisture content changes. An automatic compression-wood detection method was developed and tested on southern yellow pine lumber in the green condition. Sixteen lumber specimens were scanned using both a color camera and an X-ray scanner. Color information was shown to have significant and consistent differences between compression wood and clear wood. However, X-ray information was found to contain large density variations in green lumber due to inconsistent moisture content that would mask density variations arising from compression wood. Therefore, it was concluded that X-ray information would not be useful in detecting compression wood in green southern yellow pine lumber. A multivariate regression model was developed based only on color information from one of the board samples. A nonlinear prediction model was produced by using the original color image data and expanded variables derived from the color images. The model based on one board sample was then applied on all boards. Classified images of the board surfaces were produced and compared to manually detected compression wood. An overall accuracy of 87% was observed in the classification of compression wood.

*Keywords:* Compression wood, color scanning, X-ray scanning, nondestructive evaluation, machine vision, image processing.

## INTRODUCTION

Compression wood is a special type of tracheid cells produced by the living softwood tree in those areas exposed to excessive compressive stress during growth—for example, the lower part of the stem in a leaning tree. This type of wood has a tendency to shrink more in the longitudinal direction than normal wood when dried, due to a larger microfibril angle (Timell 1986). This tendency is often the cause of bending and warping of planks and

boards during the drying process. Sawn wood containing excessive compression wood is undesirable because of the low value and the handling problems it may cause in the sawmill process. To minimize waste production and unnecessary material handling of the wood products, compression wood should be detected and rejected at an early stage of the production, i.e., in the green condition.

Compression wood is difficult to detect visually, especially on tangential and radial wood surfaces. The most reliable way to detect compression wood is with a microscope where the special properties of the compress-

---

† Member of SWST.

sion wood cells, as round cross section, intercellular spaces, and helical cavities in lumen, can be observed (Timell 1986). On a macroscopic level, destructive testing methods are available to measure the amount of light transmitted through thin cross sections of wood since compression wood absorbs more light in the grain direction than normal earlywood and latewood. These methods can be performed manually with white light (Anon 1941; Timell 1986) or automatically using a color vision system (Andersson and Walter 1995). Non-destructive methods to detect compression wood are rare; however, techniques have been employed to separate compression wood from normal wood in the dry state by measuring the spectral reflection using an imaging spectrometer (Nyström and Hagman 1999). Since compression wood has a higher density than normal wood, it should also be possible to detect using X-ray scanning. X-rays have been used for detecting various internal defects in wood (Bond et al. 1998; Grundberg 1994; Lindgren 1992) based on density differences, and it has been shown that compression wood can be detected in dry spruce (Nyström 1998).

The overall goal of this investigation was to detect compression wood, both automatically and nondestructively, in green newly sawn boards of southern yellow pine (*pinus* sp.) (SYP). To address this goal, this study focuses on gaining a basic understanding of how compression wood appears in X-ray and color image data. The specific objectives of this study include:

1. Assess the use of X-ray and color image data for the detection of compression wood in green SYP.
2. Evaluate the accuracy of a multivariate regression model for automatically detecting the occurrence of compression wood from green SYP image data.

#### MATERIALS AND METHODS

##### *Materials*

Sixteen SYP lumber specimens used for this investigation were collected at a sawmill in

southern Virginia, USA. The lumber specimens all were 32 mm (1-¼ in.) thick and 150 mm (6 in.) wide. The length of the lumber varied from 1.6 to 2.4 m (5 to 8 ft). The boards used in this investigation were selected to contain compression wood of varying degrees at some part of the surface. All boards were scanned approximately 3 h after sawing. To minimize surface drying, the lumber was closely packed together and covered with plastic during this 3-h period.

##### *Scanning methods*

The boards were scanned using Virginia Tech's lumber scanning system (Fig. 1) (Conners et al. 1997). Scanning generated combined X-ray and color images with a cross-board resolution of 1.2 pixel/mm (30 pixel/in.) and a downboard resolution of 0.63 pixel/mm (16 pixel/in.). The X-ray and color systems were calibrated to have identical spatial resolution so that a pixel location on either image could be referenced to the same location on a lumber specimen.

*X-ray scanning.*—Scanning with X-rays gives an averaged image of the wood density throughout the lumber thickness, not only on the surface. This average wood density can be useful for detection of compression wood since it has a higher density than normal wood. The X-ray system employed an EG&G Astrophysics X-ray source with the radiation energy set to 100 keV and 0.6 mA. The X-ray sensor was a 256-pixel line array manufactured by FISCAN. The images were shade-corrected using a linear function, and the contrast was optimized by calibrating the minimum level (highest absorption) with a target of 45-mm-thick polyethylene.

It was evident after scanning the boards that compression wood was difficult to detect in green lumber with X-rays. It was found that density changes associated with moisture variations in the wood masked the smaller density changes associated with compression wood (Fig. 2). The darker regions in the green lumber X-ray image in Fig. 2a are more dense due

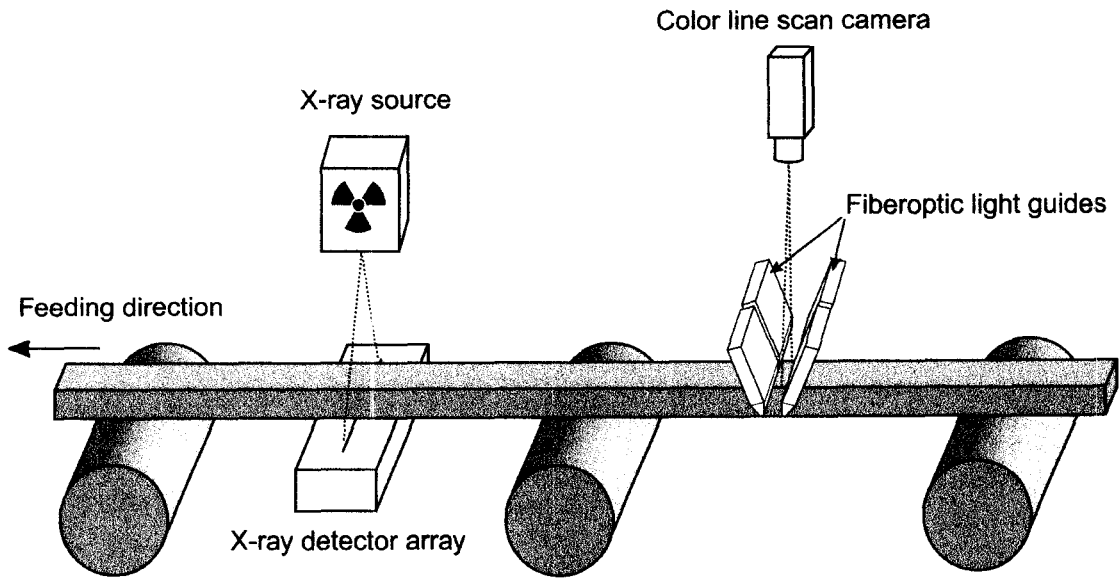


FIG. 1. Setup of the X-ray and color scanner system.

to higher moisture retained in the sapwood of SYP. After the lumber is dried, higher densities associated with moisture are removed (Fig. 2b) and compression wood can be readily observed through contrast enhanced images (Fig. 2c).

*Color scanning.*—It was observed that compression wood on the surface of the newly

sawn SYP lumber appeared as a “reddish” color. This color appearance, if significant, could be utilized for the automatic detection of compression wood using a color camera. Color images were collected using a Pulnix TL-2600 RGB line scan camera with a resolution of 864 pixels. The camera was mounted perpendicular to the wood surface, and four

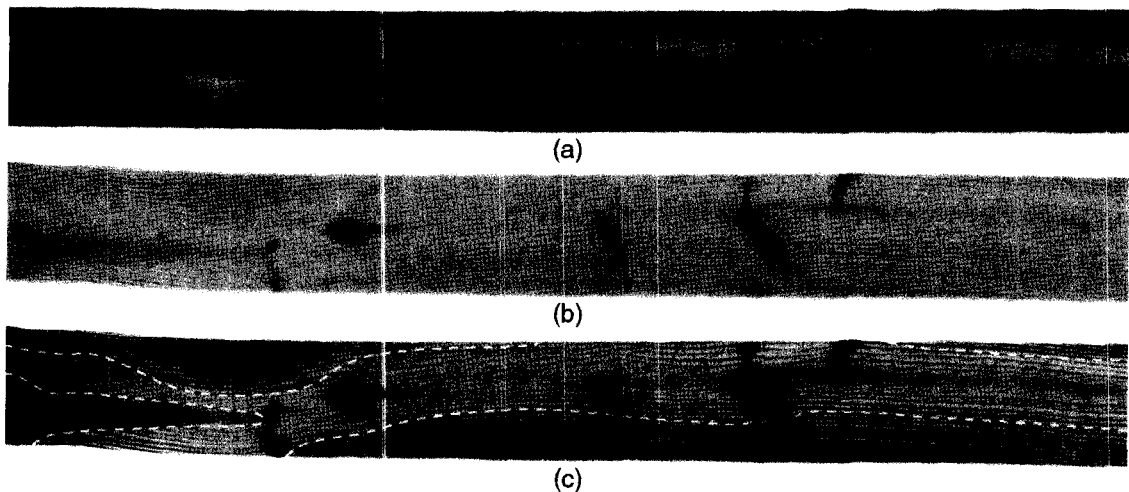


FIG. 2. X-ray images of Board 13 in green (a) and dry condition (b). Image (c) is a contrast-enhanced version of (b) with manually observed compression wood areas denoted between the dashed lines and board edges.

linear Fostec fiber-optic light lines were used to illuminate the surface of the lumber. These light lines were arranged pairwise in a small angle from the optical axis of the camera illuminating a line across the boards perpendicular to the feeding direction (see Fig. 1). The Pulnix camera has three sensor arrays filtered with red, green, and blue interference filters, respectively. This camera configuration gives a slight spatial offset of the three color images, but no undesired effects were observed for this experiment. The camera was fitted with two color-balancing filters (Schott filter numbers FG-6 and BG-34), and the three color channels were individually shade corrected with a linear function.

#### *Multivariate modeling*

As indicated earlier, the moisture content present in green SYP lumber presented problems for accurate compression wood detection using X-ray images. For color images, however, visual appraisal of compression wood noted distinct color differences from normal earlywood and latewood in the green condition. It was hypothesized that these color differences could be automatically detected and classified. Therefore, a classification model was developed using only color image data. This model was made using the MIPLS algorithm (Multivariate Image Projections to Latent Structures) (Hagman 1996) and was implemented using the public domain NIH Image software available from the National Institutes of Health (NIH 1999).

Partial Least Squares Regression Projections to Latent Structures (PLS) is a method of iteratively fitting bilinear models in several blocks of variables and can make linear regression models for many classes simultaneously. MIPLS uses the kernel algorithm for PLS (Lindgren et al. 1992), which allows many objects (such as pixels in an image) to be modeled as several classes in a fast and memory-saving way. The result of MIPLS can be displayed as prediction images after apply-

ing weight and offset coefficients on the original image data.

To separate compression wood from normal wood and all other features that normally occur in wood, a number of classes were composed. Simply dividing the features into two classes such as compression wood and non-compression wood did not work because of the large color variations of the features included in the non-compression wood class. Therefore, four subclasses were introduced for non-compression wood: latewood, earlywood, background, and knot. These subclasses were modeled as separate classes but were all considered as non-compression wood in the evaluation. Other common features in SYP such as pith, bark, and resin could also be introduced as subclasses in the model. However, modeling other non-compression wood features was not warranted in this study because occurrences of these features in the training set were minimal.

Compression wood could not easily be separated from the other classes using separate color channels or simple linear combinations of various color channels. Therefore, it was concluded that nonlinear effects needed to be incorporated in the model. Nonlinear effects were modeled by introducing nonlinear transformations of the original image data (Hagman 1996) to allow for better separation of the feature classes. In this case the original R, G, and B (red, green, and blue) images were expanded to six additional nonlinear variables:  $R^2$ ,  $G^2$ ,  $B^2$ ,  $R \times G$ ,  $R \times B$ , and  $G \times B$ . Transformation from the RGB color space to some other color representation scheme like HSI (Hue, Saturation, Intensity) has not been shown to significantly improve classification of wood features (Brunner et al. 1993; Hagman 1996). Furthermore, a color space transformation would also be time-consuming and thus undesired for an industrial implementation.

The MIPLS algorithm resulted in linear weight coefficients for each variable, and the prediction model for all classes can be written as:

$$\begin{bmatrix} \mathbf{P}_{cw} \\ \mathbf{P}_{lw} \\ \mathbf{P}_{ew} \\ \mathbf{P}_{bg} \\ \mathbf{P}_{kn} \end{bmatrix} = \begin{bmatrix} W_{cwR} & W_{cwG} & W_{cwB} & W_{cwR2} & W_{cwG2} & W_{cwB2} & W_{cwRG} & W_{cwGB} & W_{cwRB} & o_{cw} \\ W_{lwR} & W_{lwG} & W_{lwB} & W_{lwR2} & W_{lwG2} & W_{lwB2} & W_{lwRG} & W_{lwGB} & W_{lwRB} & o_{lw} \\ W_{ewR} & W_{ewG} & W_{ewB} & W_{ewR2} & W_{ewG2} & W_{ewB2} & W_{ewRG} & W_{ewGB} & W_{ewRB} & o_{ew} \\ W_{bgR} & W_{bgG} & W_{bgB} & W_{bgR2} & W_{bgG2} & W_{bgB2} & W_{bgRG} & W_{bgGB} & W_{bgRB} & o_{bg} \\ W_{knR} & W_{knG} & W_{knB} & W_{knR2} & W_{knG2} & W_{knB2} & W_{knRG} & W_{knGB} & W_{knRB} & o_{kn} \end{bmatrix} \times \begin{bmatrix} \mathbf{R} \\ \mathbf{G} \\ \mathbf{B} \\ \mathbf{R2} \\ \mathbf{G2} \\ \mathbf{B2} \\ \mathbf{RG} \\ \mathbf{GB} \\ \mathbf{RB} \\ 1 \end{bmatrix} \quad (1)$$

where **P** denotes the prediction image vector for the different classes (cw = compression wood, lw = latewood, ew = earlywood, bg = background, and kn = knot). The RGB input image vector is denoted as **R**, **G**, **B** for the original red, green, and blue images, respectively, **R2**, **G2**, **B2** are the square of each position (pixel) in the **R**, **G**, and **B** images, respectively (for example,  $r_{2,ij} = (r_{ij})^2$ , etc.), and **RG**, **GB**, **RB** are pixelwise cross multiplication between two of the original **R**, **G**, and **B** images (for example,  $rg_{ij} = r_{ij} \cdot g_{ij}$ , etc.). The matrix of weight coefficients, *w*, and offsets, *o*, describe the linear combination of the RGB input image vector that will give the prediction image vector, **P**.

The model was “trained” (e.g. the matrix of weight coefficients and offsets were estimated) on a part of Board 13 with the size  $150 \times 850 \text{ mm}^2$ , using 85,365 pixels. This part of Board 13 was chosen as the training set because of its composition of all the features to be modeled in a relatively small surface. Five classes were trained: compression wood, latewood, earlywood, background, and knots. The weight coefficients and offsets estimated by the MIPLS algorithm in the training procedure are shown in Table 1.

Using the model produced from the small training set, an implementation of the model was then made by applying the estimated

weight coefficients on the rest of the 16 boards scanned. For each board, this implementation resulted in prediction images for each of the five classes. The prediction images show the probability for class possession as grayscale value in each pixel (Fig. 3). These prediction images were then mutually compared using a simple Bayesian classifier (Duda and Hart 1973) and assigning each pixel to the class whose prediction image has the highest value in that point. The result can be displayed as classified images (Fig. 4) where the normal wood features (earlywood, latewood, and knots) are combined in a single non-compression wood class.

#### Evaluation of the classification method

The classified images were evaluated by comparing them with the real boards and judging if the areas classified as compression wood were correct. The compression wood areas were manually detected by looking for dullness, lifelessness, and lack of luster (Panshin and de Zeeuw 1980; Timell 1986) in the darker parts of the annual ring (what appears to be latewood). If the width of the darker part of the annual ring exceeds one third of the whole annual ring, it was judged as compression wood. Note that only the presence or absence of compression wood was considered in the evaluation. The performance of the model to

TABLE 1. Estimated weight and offset coefficients for all classes (see Eq. 1). Note that the weight coefficients for the expanded variables are smaller since the variables are up to 256 times larger when squared.

Weight coefficients	$W_k$	$W_G$	$W_B$	$W_{k2}$	$W_{G2}$	$W_{B2}$	$W_{RG}$	$W_{RB}$	$W_{GB}$	O (offset)
Compression wood (cw)	1.4364	1.5607	-2.1902	-0.0091	0.0046	0.0025	-0.0027	-0.0030	0.0041	79
Latewood (lw)	-0.8620	1.6132	-1.7649	0.0180	-0.0017	0.0212	-0.0016	-0.0282	-0.0038	91
Earlywood (ew)	-0.4592	-1.6970	3.3946	-0.0041	-0.0035	-0.0145	0.0020	0.0169	-0.0020	118
Background (bg)	-0.1432	0.0812	0.1971	0.0065	-0.0011	0.0010	0.0013	-0.0039	-0.0024	65
Knots (kn)	-0.7758	-1.3340	0.8605	-0.0010	-0.0007	-0.0022	0.0013	0.0085	0.0014	79

detect other features was not evaluated; they were only included in the model to better explain the large variability of wood.

The surfaces of all boards were evaluated, and every pixel was judged to be either correctly classified normal wood, correctly classified compression wood, false positive classification or false negative classification (Table 2). False positive classification is normal wood area misclassified as compression wood. False negative classification is compression wood area misclassified as normal wood. The four other classes (latewood, earlywood, background, and knots) were all considered as non-compression wood or "normal wood" areas in this evaluation.

#### RESULTS AND DISCUSSION

In this study, X-ray scanning was found an inappropriate method to detect compression wood in green SYP. The water in the wood was found to highly dominate the density of the green boards and thus hide the smaller density differences caused by the compression wood. The distribution of the moisture in the wood was very irregular (Fig. 2). X-rays are attenuated in different materials depending on their chemical composition and mass. The difference in X-ray mass attenuation between wood and water is very small at the energy used (Lindgren 1992), which means that the density effects of wood and water can not be easily separated in an X-ray image. Hence, single energy X-ray scanning such as the one used in this scanning system cannot be used to classify compression wood in green SYP lumber.

Compensation of X-ray images to remove moisture effects was not possible since the moisture in green SYP is far from uniformly distributed (see Fig. 2). Furthermore, density variations attributed to moisture content and compression wood are difficult to separate. Compression wood has a higher density than normal wood in dry condition due to its thicker cell walls. This higher density means that the tracheid lumen is smaller (the wood is less porous) and can not fill with the same amount of water as normal wood can above the fiber

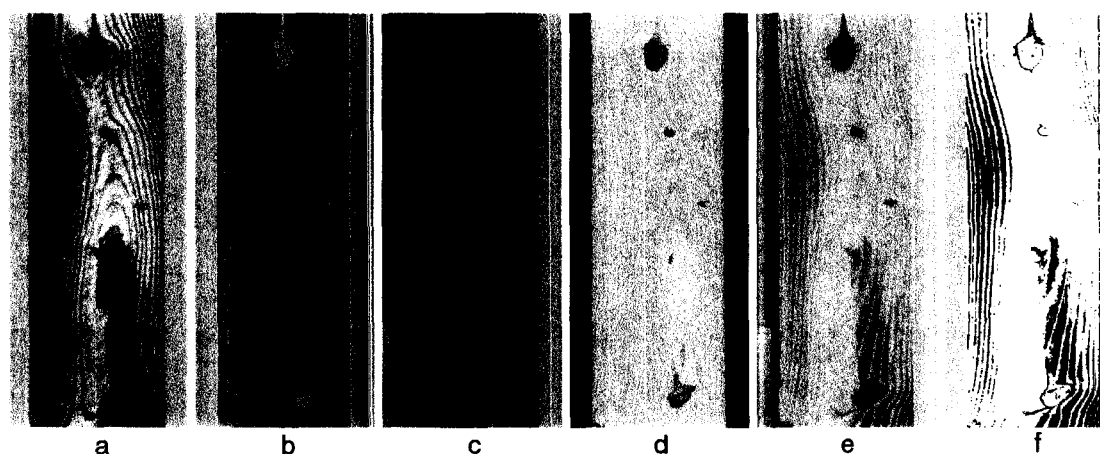


FIG. 3. Prediction images (a–e) and a classified image (f) of the training set, a portion of Board 13. The prediction images show the probability for class possession, dark = high probability, light = low probability. Letters denote: a = compression wood, b = latewood, c = earlywood, d = background, e = knots. The classified image shows normal wood features (earlywood, latewood, and knots) as white, compression wood as black, and background as gray.

saturation point, i.e., green compression wood can be drier than normal green wood. Therefore, density differences in compression wood are further masked and even harder to detect with X-rays in the green condition.

Color scanning with an RGB camera worked well for detecting compression wood in the green state. The compression wood has a predominant reddish color in the green state that made it easier to detect than after drying. A possible explanation is that the free water in the lumber helps the light to penetrate deeper in the wood surface and thus get more influence from the light-absorbing characteristics of the wood, i.e. the color contrast is stronger in wet wood.

The multivariate model for detecting compression wood was made with MIPLS, using only the color images from a part of Board 13 as input data. The original R, G, and B variables were expanded to  $R^2$ ,  $G^2$ ,  $B^2$ ,  $R \times G$ ,  $R \times B$ , and  $G \times B$ , which made the model nonlinear. Five different classes were used in the model: compression wood, latewood, earlywood, background, and knots. Weight coefficients produced by MIPLS for all classes and variables are shown in Table 1.

The model was made using only a part of one board as the training set. This small train-

ing set can result in overfitting. Such overfitting can limit the model's applicability for a larger batch of boards, which can have variability that has not been described by the training set. Better classification models can be made by carefully understanding the color variability in SYP lumber and then selecting representative training sets. In this investigation, there were only five classes of wood features modeled. Other common features in SYP were not included because they were not present to a sufficient extent in the 16 lumber specimens studied. If other features such as pith, resin, and surface stains are prevalent in lumber, then their subclassification and inclusion in the training set may be required for improved classification performance.

An evaluation of the performance of the model was made by comparing the classified images to a manual judgment of the same boards. Only the compression wood was considered in this evaluation, and all other classes were thought of as non-compression wood. The average correct compression wood classification was found 89%. Further, 14 of the 16 boards (87.5%) evaluated had more than 85% correct classification of the board surface, which can be regarded as satisfactory. The result for all boards is shown in Table 2.



FIG. 4. Grayscale images (left) compared to classified images (right) for Boards 8, 12, and 13, respectively. Note that Board 12 has a different appearance from the other two, which might explain the lower classification accuracy for that board.

In this study, there was no possibility to manually classify compression wood with the same resolution as the scanning system, and a manual classification is always subjective. This mismatch of resolution and subjectivity

can cause small errors in the evaluation result, but the method should still give a good indication of the trends in the performance of the system.

As mentioned earlier, 14 of the boards were

TABLE 2. Evaluation results. Calculated values are in percent of board area.

Board number	Board area (pixel)	Classified compression wood	False positive compression wood	False negative compression wood	Manually estimated compression wood	Correct classified board area
1	188,964	24.3%	0.8%	3.1%	26.6%	96.1%
2	296,495	25.6%	5.3%	0.8%	21.1%	93.9%
3	226,886	36.6%	11.3%	1.7%	27.1%	87.0%
4	302,010	16.1%	3.6%	0.9%	13.4%	95.5%
5	250,228	22.8%	7.4%	0.6%	16.1%	92.0%
6	183,555	10.5%	6.3%	1.0%	5.2%	92.7%
7	234,125	39.3%	3.5%	0.0%	35.8%	96.5%
8	289,042	26.6%	5.1%	4.9%	26.4%	90.0%
9	266,202	36.5%	31.8%	0.0%	4.6%	68.2%
10	188,299	10.2%	7.0%	7.6%	10.8%	85.4%
11	228,254	10.3%	0.2%	11.2%	21.2%	88.6%
12	284,553	39.3%	38.3%	0.0%	1.0%	61.7%
13	290,542	15.0%	1.4%	2.1%	15.8%	96.5%
14	185,051	28.1%	3.0%	0.3%	25.4%	96.6%
15	263,697	5.4%	3.6%	1.8%	3.6%	94.6%
16	239,574	20.7%	4.6%	3.2%	19.3%	92.2%
Total	3,917,477	23.2%	8.8%	2.3%	16.8%	88.9%

classified as acceptable. It was observed that most of the false positive detection errors found in these 14 boards were located in areas surrounding knots. Some of the darker-colored latewood areas were also misclassified as compression wood. These areas tend to have similar color characteristics as compression wood for the samples tested. The two other boards with bad classification results (Boards 9 and 12, Table 2) were notably different from the others by having many knots and more resinous wood. Figure 4 shows grayscale and classified images of Board 12 in comparison to Boards 8 and 13, where some differences in appearance can be observed. Board 8 is similar in nature to the training sample (Board 13) and has good classification accuracy (90%), while Board 12 is notably different (e.g., large frequency of knots and a generally darker appearance) and has a lower accuracy (62%). This notable difference indicates that the performance of the system can be improved by carefully selecting the appropriate training set when estimating MIPLS coefficients.

The classification technique described here can easily be implemented in a scanning system using RGB color cameras, and even in existing systems, by further processing of the

color images according to the resulting model. Considering the simplicity of the model, it can be processed pixelwise in real time while the image is collected, preferably done by a hardware implementation to speed up the processing. However, the model presented here is valid for only the system on which it was trained. Any new implementation of the technique must always be calibrated and trained for the specific system using the procedures described earlier.

It is important to note that the classification results found in this study are preliminary based on a small sample of SYP lumber. These preliminary results show that certain color characteristics in green lumber correlate strongly with regions of compression wood. However, before a practical industrial scanning system can be developed, further work is needed to quantify how color characteristics found in compression wood overlap with all other noncompression wood features. This work would be necessary for designing an optimum training sample and for determining whether other scanning and image processing techniques would be necessary for an industrially robust detection system. In working towards such a system, this study has provided

a first step in understanding how SYP compression wood appears in X-ray and color images.

#### CONCLUSIONS

Significant findings gained from this study include:

1. Density differences in compression wood are masked by density variations associated with moisture content making it difficult to detect in the green condition with single-energy X-ray imaging systems.
2. Compression wood has a predominant reddish color in the green condition indicating that RGB color images can be useful in nondestructive detection of compression wood. Incorporating color information into a multivariate regression model resulted in an overall compression wood classification accuracy of over 87%.
3. Compression wood could not easily be separated from non-compression wood using separate RGB color channels or linear combinations of these channels. Nonlinear combination of these color channels were necessary for more complete and accurate separation.
4. Compression wood could not be simply separated using only 2 classes: compression wood and non-compression wood. Non-compression wood had to be further subclassified as latewood, earlywood, knots, and background to more accurately model separations in color variability found in the tested images.
5. False compression-wood detection errors arose predominantly in areas surrounding knots and darker colored latewood areas. These areas tend to have similar color characteristics as compression wood for the samples tested.

#### REFERENCES

- ANDERSSON C., AND F. WALTER. 1995. Classification of compression wood using digital image analysis. *Forest Prod. J.* 45(11/12):87-92.
- ANONYMOUS 1941. 1953. A simple device for detecting compression wood. US Forest Service FPL, Rep. 1390., Madison, WI.
- BOND, B. H., D. E. KLINE, AND P. A. ARAMAN. 1998. Characterization of defects in lumber using color, shape, and density information. Pages 581-587 in *Proc. International Conference on Multisource-Multisensor Information Fusion*, CSREA Press.
- BRUNNER C. C., A. G. MARISTANY, D. A. BUTLER, AND J. W. FUNCK. 1993. Enhancing color-image data for wood-surface feature identification. *Proc. 5th Int. Conf. on Scanning Technology & Process Control for the Wood Products Industry*. Atlanta, GA.
- CONNERS R. W., D. E. KLINE, P. A. ARAMAN, AND T. H. DRAYER. 1997. Machine vision technology for the forest products industry. *Computer* 30(7):43-48.
- DUDA R., AND P. HART. 1973. *Pattern classification and scene analysis*. John Wiley & Sons, New York, NY.
- GRUNDBERG S. 1994. Scanning for internal defects in logs. Licentiate thesis, Luleå University of Technology, Luleå, Sweden.
- HAGMAN O. 1996. On reflections of wood. Ph.D. thesis, Luleå University of Technology, Luleå, Sweden.
- LINDGREN O. 1992. Medical CT scanners for non-destructive wood density and moisture content measurements. Ph.D. thesis, Luleå University of Technology, Luleå, Sweden.
- , P. GELADI, AND S. WOLD. 1992. The kernel algorithm for PLS. *J. Chemometrics* 7:45-59.
- NATIONAL INSTITUTES OF HEALTH (NIH). NIH Image Version 1.62. April 1999. <http://rsb.info.nih.gov/nih-image/> (14 June 1999).
- NYSTRÖM J. 1998. Detection of *Picea abies* compression wood with a multisensor system. *Proc. 3rd International Seminar/Workshop on Scanning Technology and Image Processing on Wood*. Luleå University of Technology. Technical Report 1998:27.
- , AND O. HAGMAN 1999. Real-time spectral classification of compression wood in *Picea abies*. *J. Wood Science* 45(1):30-37.
- PANSHIN A. J., AND C. DE ZEEUW. 1980. *Textbook of wood technology*. 4 ed. McGraw-Hill, New York, NY.
- TIMELL T. E. 1986. *Compression wood in gymnosperms*. Springer Verlag, New York, NY.